High accuracy image classification through preprocessing and dimensionality reduction applied to melanoma detection[1]

Mauricio Y. Chigutti[2,3], Carlos H. Q. Forster[3], Felipe S. L. G. Duarte[2]
[2]Data Science Team, Itaú Unibanco, São Paulo, Brazil. Email:{mauricio.chigutti, felipe.duarte}@itau-unibanco.com.br
[3]Computer Science Division, Instituto Tecnológico de Aeronáutica, São Jose dos Campos, Brazil. Email: forster@ita.br

***Abstract*—Melanoma, one of the most prevalent human cancer disease, presents increased survival rate when early detected. Deep Convolutional Neural Networks (CNN) demonstrates high potential in fast and automated skin lesion classification; nevertheless, it is a complex task to differentiate melanoma from the potential skin lesions, given the visual similarities between the possible diagnoses. In order to improve classification capacity, we implement a series of image transformations, feature extraction by the transfer of knowledge from pre-trained neural networks and a non-linear projection in attribute space using an auto-encoding technique. We test the performance of the resulting architecture on the public ISIC 2017 dataset, achieving 0.89 area under the ROC curve for the melanoma classification task.**

Keywords—skin lesion classification, deep learning, convolutional neural networks, auto-encoder.

I. Introduction

Dermatologists have been using and recommending extensively the ABCDE technique [27] towards melanoma detection early detection. This exam consists of visual inspecting skin lesions in order to identify asymmetry and observe border, color, diameter and evolution. This technique demands specialists knowledge and is susceptible to human biases and the observer variations. Since melanoma is one of the deadliest forms of skin cancer, with approximately 75% of all skin cancer countable deaths, early detection, which the visual inspections, in most cases, accomplish primarily, is essential for higher survival rates.

Training experts that can efficiently identify skin cancer by visual inspection is time expensive. Therefore, specialists have been exploring digital dermoscopic images for more automated lesion classification. Dermoscopy consist in taking magnified images of skin lesion regions with enhanced illumination and resolution to facilitate the analysis of the skin area in study. These images not only intensify the lesion characteristics, but also highlights other non-desirable skin features, such as skin color, hairs and veins. This effect may hinder the identification of melanoma from benign lesions.

In order to circumvent these recognition difficulties, we approach preprocessing of digital images to improve their final classification. Extensive studies [1-5] have shown that lesion segmentation can improve melanoma detection by removing the noisy part of the skin containing features that does not belong primarily to the lesion. However, segmentation can remove important parts of the lesion that contrasts with the skin. This may produce weak color identification towards melanoma. In addition, Barata et al. [6] and Cherepkova et al. [7] explore the effects of color correction and contrast enhancement to improve skin cancer detection. Another method explored broadly in the skin lesion classification problem is the usage of hand-crafted Convolutional Neural Networks (CNN) [8] and pre-trained CNN [10][12] for feature extraction of malignant and benign lesions. The International Skin Imaging Collaboration (ISIC) hosts competitions since 2016 that aim the differentiation of skin lesion diagnosis, rewarding the best machine learning algorithms capable of better segmenting and classifying the different types of skin lesions. These algorithms are often ensembles of pre-trained ImageNet networks.

This paper proposes an automated melanoma classification method using dermoscopic images with a different CNN architecture from the previous cited works, comprised of a multimodal feature extraction from different images transformations and auto-encoding dimensionality reduction. A multimodal approach requires different sources for the CNN to learn distinct features from the lesions and facilitate the melanoma detection. The diverse sources adopted in this paper are from preprocessing techniques such as Gray Word color constancy [23], histogram equalization algorithm Contrast Limited Adaptive Histogram Equalization (CLAHE) [22] and lesion segmentation, as well as the original image. We obtained these features from the pre-trained Google's network Inception-v3 [11] to generate a concatenated vector of attributes with different lesion properties. Then, the features undergo dimensionality reduction by a two-layer auto-encoder as shown in Figure 1, improving the performance of the previous CNN.

The highest score area under the Receiving Operating Characteristic (ROC) curve (AUC) we achieved with a single Inception-v3 is 0.87, which matches the best score in the 2017 ISIC competition for melanoma detection with a public dataset. Moreover, the dimensionality reduction evidenced a gain in a compressed feature representation, outperforming the AUC score from 0.87 to 0.89. The remainder of the paper is organized as follows: in Section II a brief review of melanoma classification works is presented. In Section III, we describe the dataset chosen. In section IV, we describe the preprocessing and data augmentation algorithms. In Section V the training strategy and experimental results are explained. Section VI we derive the conclusions.

II. Related Work

The classification of skin lesion has been the subject of many papers, varying mostly in the preprocessing adopted, the segmentation algorithm and CNN design. Dorj et al. [10] extracted image features with the AlexNet pre-trained network and classified different skin lesions through an SVM algorithm, reporting a 94.2% accuracy in a melanoma dataset acquired from Google images. They focused on tuning the parameters of the convolutional layers, maxpooling layers and fully connected layers, besides the validation of the SVM

[1] Any opinions, findings, and conclusions expressed in this manuscript are those of the authors and do not necessarily reflect the views, official policy or position of Itaú-Unibanco.

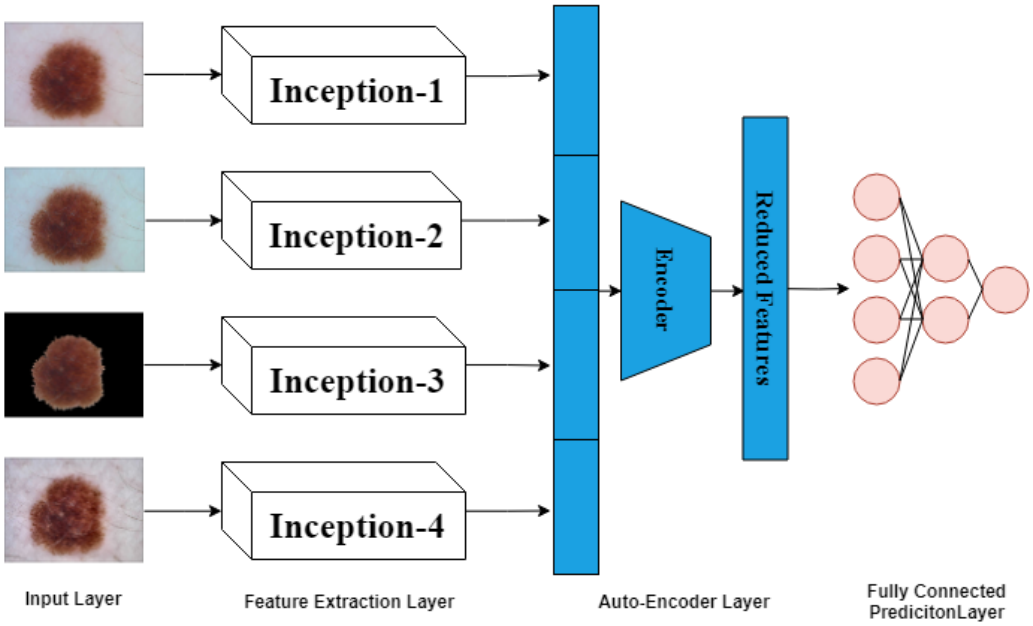

Fig. 1 – Proposed architecture for melanoma classification. The input layer receives three pre-processed images and the original image. Each image undergoes an Inception-v3 CNN, which comprises the feature extraction layer. We concatenated the resulting vector in a single layer and trained in the auto-encoder process for dimensionality reduction. Then we combined the output of the encoder in a fully connected layer to produce the final prediction in the melanoma classification.

algorithm and cropping of the raw images. Esteva et al. [12], using the Inception v3, fine-tuned the CNN with 129,450 images in 2032 skin lesion categories and reported a 0.94 AUC for dermoscopy melanoma images. Their goal was to compare dermatologists performance in identifying carcinoma and melanoma against the proposed CNN algorithm. Similarly, Haenssle et al. compared 58 dermatologists diagnostic capability, achieving a mean value of 0.86 AUC, higher than the score the experts could achieve.

Gutman et al. [14] adopted a slightly different solution specifically to the melanoma classification problem. Even though the AlexNet network was the main feature extractor of the skin lesions, they also created custom handcrafted features from the ISIC 2016 competition dataset. With these new vector, the authors predicted melanoma and non-melanoma lesions with a SVM algorithm reporting 0.804 AUC score. Some publications favored an ensemble architecture of decision, training several CNNs models in parallel and averaging their outputs in some form. Kawahara et al [15] varied the image resolution of the same image as input for different pre-trained CNNs, concatenating their outputs and using as an input for a previous fully connected network prediction layer. In addition, a set of publications explore non-neural network model approaches as well. Anas et al. [16] has segmented melanoma and non-melanoma lesions with k-means clustering by creating groups of similar luminance, color and texture. Abbas et al. [17] opted for an adaptative boosting algorithm AdaBoost MC achieving high AUC score and similar result as dermatologists interviewed.

Preprocessing and segmentation of dermoscopy images is a crucial part in the classification of skin lesions problem, being the subject of several studies and reported increase in the capacity of machine learning algorithms to differentiate the possible diagnosis. Since one of the most important characteristics of malignant skin lesion is the coloration of the close region, it is reasonable to assume that color space transformation in the raw images can assist in the disease classification. Almansour [18] extracted color features from six different representation spaces like RGB, RGB, HSV, YCbCr, NTSc, CIE L*u*v and CIE L*a*b. Barata et al. [6] compared Gray World, max RGB, Shades of Gray and General Gray World color constancy algorithms, showing that such transformations can improve the sensitivity to about 8% when compared to raw images. Another common preprocessing step is the removal surrounding skin and hair, leaving only the segmented lesion. Analogously to the color, the shape and border of the lesion generally present higher variance when compared between benign and malignant moles, the second being more rough and irregular. Lin et al. [1] concerned themselves solely with the quality of the segmentation comparing a U-net and clustering approach. Other works, including Yuexiang and Shen [8], utilize the segmentation as an essential prior step for the classification.

The previous papers mentioned inspired the architecture of the CNN designed in this paper is by extracting the features from the raw image, the image of a Gray World transformation, the segmented image and the image with a histogram equalization for enhanced contrast. Ding and Tao [18] that concatenated features extracted from patch images and 3D transformation of facial representation and performed a stacked auto-encoding algorithm (SAE) for feature reduction influenced the method proposed for the auto-encoding layer.

III. Dataset

The papers on skin lesion classification are not consensual regarding dataset selection. Each author utilizes a different dataset and some with private dermoscopy image. To confront this problem, our data was extracted from the “ISIC 2017 and 2018: Skin Lesion Analysis Towards Melanoma Detection” grand challenge datasets [20][21], which hold a competition with the best scores for the classification of melanoma listed

in their website. It comprises 2,720 images for training, 108 for validation and 510 for test, divided according to Table I.

TABLE I
ISIC DATASET DISTIBUTION BETWEEN MALIGNANT MELANOMA SKIN LESION AND BENIGN NEVUS.

ISIC Dataset		
Dataset type	***Melanoma***	***Nevus***
Train	1,348	1,372
Validation	30	78
Test	117	393

The training set consist of the original dataset for the ISIC 2017 competition with the addition of melanoma images from the HAM10000 [20] dataset of the 2018 competition. The validation and the test sets were unaltered, except by the removal of seborrheic keratosis that is not in the scope of the paper. It only considers the nevus, for example in the first row of Figure 2, and melanoma, the second row, lesions for classification as a binary problem.

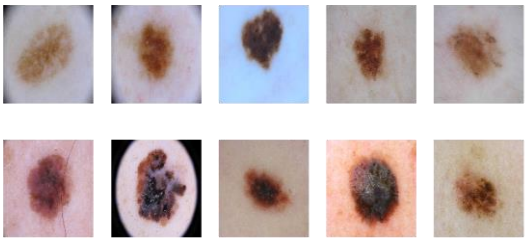

Fig. 2 – The first row contains example of benign nevus lesion and the second melanoma of the training set.

IV. PREPROCESSING AND DATA AUGMENTATION

The total dataset has more than 3,000 images, varying in resolution, contrast and illumination. Before training the complete CNN architecture, we applied four preprocessing techniques to the images, Gray World and CLAHE color transformation, lesion segmentation and data augmentation. We consider these steps essential to extract the main features involving color lesion shape that are concatenated and reduced via auto-encoding.

A. Gray World

It is a simple algorithm to normalize illumination in an image. It considers that each component of a RGB color space $\boldsymbol{e} = (e_R, e_G, e_B)^T$ has an achromatic reflectance average under a natural light. This way, given a color channel $C \in \{R, G, B\}$, the average color can be computed as

$$\int f_C(x)dx = ke_C \tag{1}$$

where k is chosen that $\boldsymbol{e}$ has a unit length. The algorithm can only transform each channel separately [23]. In addition, it considers that most of the images needs correction, resulting in a white coloration impression as shown in Figure 3.

B. CLAHE

Pisano et al. [24] showed that histogram equalization methods to enhance color contrast are a valuable resource in medical images preprocessing. Lin et al. [1] demonstrated the benefits of this transformation to aid the segmentation of the lesions when compared to non-equalized images. CLAHE is an adaptation of traditional histogram equalization methods,

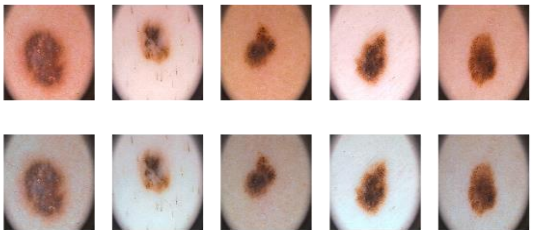

Fig. 3 – Dermoscopy images of the training set before, first row, and after the Gray World transformation.

finding a mapping for each pixel based on their local neighbors in a grayscale distribution [25]. For this process, we have to divide the image in a given grid, in our case 8x8, and converted from RGB to grayscale and back. In addition, the OpenCV library exploited for this transformation has also contrast limiting to avoid noise amplification, since the algorithm is unsupervised and cannot distinguish the main image parts from the noise.

This operation performs a set of transformations that can exaggerate image deformities and generate information loss due to the 3 to 1 channel transformation and vice versa. Considering that it is one of the four input in the proposed architecture, the other transformations attenuated the noises it can produce. In general, the CLAHE generated an inverse product of the Gray World that evenly whiten the images, by enhancing the lesion colors and skin particularities as can be seen in Figure 4.

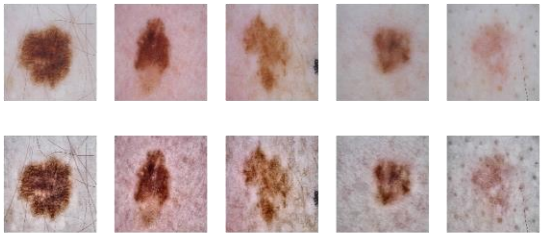

Fig. 4 – Dermoscopy images of the training set before, first row, and after the CLAHE transformation.

C. Segmentation

The task of segmentation has two main functions in the purposed architecture, to evidence the border differences between benign nevus and melanoma, and to remove skin and hair, considered noisy, from the dermoscopy image. In [1] and [8] a variety of supervised segmentation were analyzed and compared, given that the ISIC database also have a border grounding truth for this task. However, the dataset considered in this paper has additional images from the ISIC archive in the training set and we can use a more generic segmentation, since this is a fourth of the features extracted from the images. Therefore, we chose the unsupervised watershed transformation [26] for the task.

The watershed transformation is a region-based algorithm that searches for pixel similarities in a given area. It consider the image as a topographic surface with the high peaks and minimum valleys extracted from color intensity variation. The algorithm fills the identified valleys with black pixels, leaving the peaks as white pixels, simulating a flooding process. This approach can over segment and remove important part of the lesion due to noise or unwanted high intensity color

differentiation of pixels in the image. Figures 5 and 6 demonstrate the result for benign lesions and melanoma images respectively. It is possible to notice that most of the hair and skin was removed, leaving the lesion and small noisy marks along the image. In addition, it makes more visually evident the roughness of malignant lesions after the transformation.

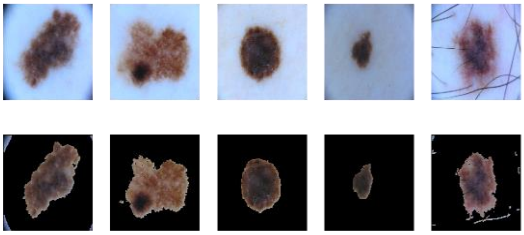

Fig. 5 – Dermoscopy images of benign nevus segmentation.

Fig. 6 – Dermoscopy images of melanoma segmentation.

D. Data Augmentation

The training set was augmented with random horizontal flip, zooming of a 0.2 percent range, horizontal and vertical shifting in a 0.2 range and rotation from 0º to 90º. For the shifting part, we filled the image block lacking information with the nearest known pixel. We consider this data augmentation process important to generate small variations in the training process in order to avoid overfitting.

V. Training Strategy and Experimental Results

The first part of the training was defining the feature extraction layer in Figure 1. Many researches in skin lesion classification benefited from transfer leaning networks [10][12][15-18] for feature extraction, varying the fully connected predication layer and architecture. Yuexiang and Shen [8] compared the performance of VGG-16 [28], ResNet50 and ResNet-101 [29], AlexNet [30] and Inception-v3 in order of best AUC achieved. We tested the first two and the last CNNs by changing the number of hidden layers and neurons in the fully connected part of the network, the activation function in each layer, the dropout rate, the learning rate and class weight in the loss function for melanoma and benign nevus. In addition, we changed the number of layers with frozen weights in a fine-tuning process, since we imported them from the ImageNet weights; Chollet [9] recommends retraining part of the CNN to make them more fitted for the given problem.

We performed this task four times, one for each input image, for the three mentioned CNNs, and we reported the best results in Table II. We show that the Inception-v3 excels in all the image inputs and, therefore, we adopted them for the final architecture. After choosing and fine-tuning the CNNs for the feature extraction layer, we removed the added prediction neurons, leaving the average global pooling as the final layer in each CNN. We adopted the notation of Ding and Tao [19], which denotes the feature extracted from each CNN as $x_i \in \mathbb{R}^d$, where $1 \leq i \leq 4$ and d, in this paper, is equal to 2048, the number of features for each Ineption-v3. Then, a network layer concatenates the features of the four CNNs, forming a large vector:

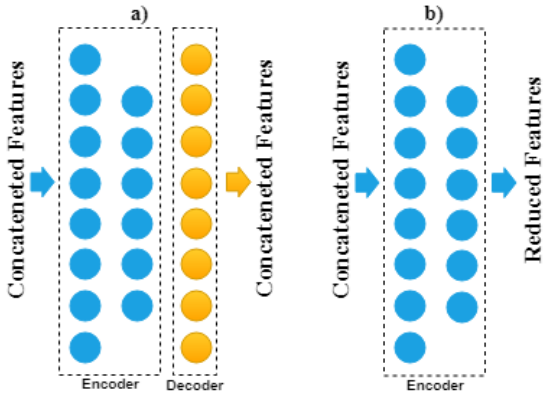

Fig. 7 –a) Auto-encoder trained to recover the concatenated features from the Inception-v3 CNNs with an input layer of 8192 neurons and an encoder layer of 2048 neurons. b) The resulting encoder that reduce the concatenated features dimension in a four time factor utilized as the input of the fully connected prediction layer.

$$\dot{x} = [x_1; x_2; x_3; x_4] \in \mathbb{R}^{4dx1} \quad (2)$$

Considering that $\dot{x}$ is four times the dimension of a single Inception-v3 output and some features might not be essential to the prediction, a compression auto-encoding method was applied inspired by [19]. The dimensionality reduction in this scenario is similar to the PCA algorithm, with the exception that the auto-encoder can capture non-linear relation between the original data and the reduced projected feature space [31]. In Figure 7a, we demonstrate the two-layer auto-encoder training part, which receives as input the 8192 features concatenated, followed by a 2048 neurons layer and a batch normalization function, representing a compression factor of four times. The activation function of this last layer is a non-linear ReLU, which is a rectifier function with the expression:

$$\phi(x) = \max\{0, x\} \quad (3)$$

The auto-encoder is trained to recover the $\dot{x}$ with mean absolute error (MAE) loss function and early stop by the loss in the validation set. Since the feature recovered can be any positive number, the decoder last layer also has a ReLU activation function. The minimum MAE achieved in the validation set was 0.0653.

TABLE II
Best Reported AUC for the VGG-16, ResNet-50 and Inception-v3 after the fine tuning.

	Reported AUC for each CNN			
CNN	***Raw Image***	***Grey World***	***CLAHE***	***Segmented Image***
VGG-16	0.82	0.76	0.78	0.65
ResNet-50	0.84	0.83	0.76	0.70
Inception-v3	0.86	0.87	0.80	0.73

After training the auto-encoder and defining the encoder weights, we removed the decoder part, as shown in Figure 7b, leaving only the reduced features as the encoder output. We

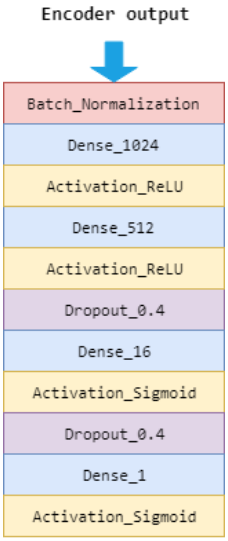

Fig. 8 – Fully connected prediction layer of the final CNN architecture.

added a fully connected layer for the final prediction to the encoder and performed a set of tests with batch normalization, the number of dense neurons, the number of hidden layers, the leaning rate, the activation function in each layer and the dropout rate. We compared each of the tested prediction layers, resulting in the architecture with the lowest binary cross-entropy loss function value demonstrated in Figure 8.

The metrics we considered for the evaluation of each individual Inception-v3 and the final CNN, comprised of the previous Inceptions with the auto-encoding layer and fully connected prediction layer as exhibited in Figure 1, are the AUC, accuracy (ACC), sensitivity (SE) and specificity (SP). Taking N_{tp}, N_{tn}, N_{fp} and N_{fn} as the count of true positive, true negative, false positive and false negative, respectively, and considering the melanoma as the target label, we defined them as:

$$ACC = \frac{N_{tp}+N_{tn}}{Total}, SE = \frac{N_{tp}}{N_{tp}+N_{fn}}, SP = \frac{N_{tn}}{N_{tn}+N_{fp}} \quad (4)$$

In Table III, we expose the resulting performance of the final architecture and each Inception-v3, named Incep-RAW, Incep-GW, Incep-CLAHE and Incep-SEG for the respective inputs raw, Gray World, CLAHE and segmentation. There is a gain in the AUC from the Incep-GW, the best solo performing CNN, of 0.2 points and a 0.1 accuracy increase from the Incep-RAW.

TABLE III
PERFORMANCE OF THE HIGHEST SCORED FINE-TUNNED CNNS FOR SKIN LESION PREDITICTION AND FINAL ARCHITECTURE.

Results				
CNN	***AUC***	***ACC***	***SE***	***SP***
Incep-RAW	0.86	0.84	0.67	0.90
Incep-GW	0.87	0.82	0.63	0.89
Incep-CLAHE	0.80	0.81	0.33	0.96
Incep-Seg	0.73	0.74	0.52	0.81
Final Architecture	0.89	0.85	0.66	0.91

In Figure 9, the ROC curves demonstrate a slight detachment of the final architecture in comparison with the best CNNs before the auto-encoding step. The peak in the final

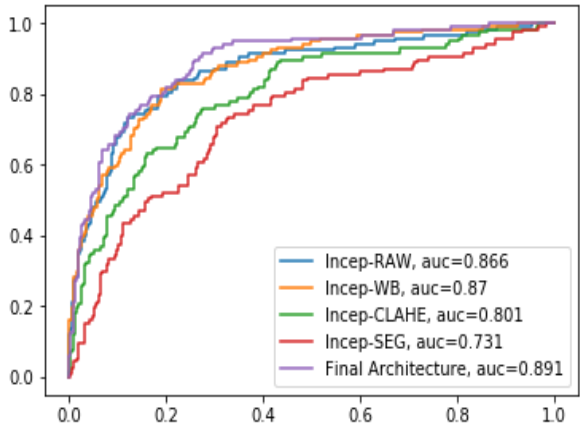

Fig. 8 – ROC curve and the respective AUC for each CNN.

architecture indicates a threshold of approximately 0.25 for highest melanoma detection, resulting in a 0.71 SE.

VI. CONCLUSIONS

Melanoma recognition in computer vision applications is a challenging task given the similarity between benign and malignant lesions. We approach this problem by creating a multimodal deep architecture with three distinct preprocessed and the raw cropped image as inputs. First, we apply color enhancing (Gray World), histogram equalization (CLAHE) and segmentation in the original image, enhancing the characteristically diagnosis features. Second, we fine-tune pre-trained Inception-v3 networks for molded feature extraction. Third, we apply non-linear dimensionality reduction by auto-ending the concatenated extracted features by a four time encoded space. Finally, we combined and extensively tested a new fully connected layer to achieve the final architecture.

The results indicate a slight increase in performance from single pre-trained adjusted CNNs with the feature dimensionality reduction, culminating in a 0.2 gain from the highest AUC score achieved. This score of 0.89 AUC, also, outperforms the best competitor displayed score in the ISIC 2017 competition for melanoma classification, indicating a potential in multimodal leaning framework for lesion classification. As future work, the architecture of the final proposed model can be adapted to accommodate others lesions diagnosis in a multi-classification problem.

REFERENCES

[1] B. S. Lin, K. Michael, S. Kalra and H. R. Tizhoosh, "Skin lesion segmentation: U-Nets versus clustering," 2017 IEEE Symposium Series on Computational Intelligence (SSCI), Honolulu, HI, 2017, pp. 1-7.

[2] H. Ozkan, R. Gurleyen, E. Usta and R. K. Kumrular, "Automatic skin lesion segmentation," 2017 Electric Electronics, Computer Science, Biomedical Engineerings' Meeting (EBBT), Istanbul, 2017, pp. 1-3.

[3] S. Joseph and J. R. Panicker, "Skin lesion analysis system for melanoma detection with an effective hair segmentation method," 2016 International Conference on Information Science (ICIS), Kochi, 2016, pp. 91-96.

[4] S. Ross-Howe and H. R. Tizhoosh, "The Effects of Image Pre- and Post-Processing, Wavelet Decomposition, and Local Binary Patterns on U-Nets for Skin Lesion Segmentation," 2018 International Joint Conference on Neural Networks (IJCNN), Rio de Janeiro, 2018, pp. 1-8.

[5] L. Bi, J. Kim, E. Ahn, D. Feng and M. Fulham, "Semi-automatic skin lesion segmentation via fully convolutional networks," 2017 IEEE 14th

International Symposium on Biomedical Imaging (ISBI 2017), Melbourne, VIC, 2017, pp. 561-564.

[6] C. Barata, M. E. Celebi and J. S. Marques, "Improving Dermoscopy Image Classification Using Color Constancy," in IEEE Journal of Biomedical and Health Informatics, vol. 19, no. 3, pp. 1146-1152, May 2015.

[7] O. Cherepkova and J. Y. Hardeberg, "Enhancing dermoscopy images to improve melanoma detection," 2018 Colour and Visual Computing Symposium (CVCS), Gjøvik, 2018, pp. 1-6.

[8] Li, Yuexiang and Linlin Shen. “Skin Lesion Analysis towards Melanoma Detection Using Deep Learning Network.” Sensors (2018).

[9] Francois Chollet. 2017. Deep Learning with Python (1st ed.). Manning Publications Co., Greenwich, CT, USA.

[10] Dorj, Ulzii-Orshikh, Keun-Kwang Lee, Jae-Young Choi, and Malrey Lee. "The skin cancer classification using deep convolutional neural network." Multimedia Tools and Applications 77.8 (2018): 9909-9924.

[11] Szegedy, Christian et al. “Rethinking the Inception Architecture for Computer Vision.” 2016 IEEE Conference on Computer Vision and Pattern Recognition (CVPR) (2016): 2818-2826.

[12] Kuprel, Brett, Susan M. Swetter, Helen M. Blau, Andre Esteva, Brett Kuprel, Roberto A. Novoa, and Sebastian Thrun. "Dermatologist-level classification of skin cancer with deep neural networks." Nature 542.7639 (2017): 115-118.

[13] Haenssle HA et al: "Man against machine: diagnostic performance of a deep learning convolutional neural network for dermoscopic melanoma recognition in comparison to 58 dermatologists." Annals of oncology : official journal of the European Society for Medical Oncology, vol. 29, no. 8, 2018, pp. 1836-1842

[14] Gutman, David & Codella, Noel & Celebi, M. Emre & Helba, Brian & Marchetti, Michael & Mishra, Nabin Kumar & Halpern, Allan. (2016). Skin Lesion Analysis toward Melanoma Detection: A Challenge at the International Symposium on Biomedical Imaging (ISBI) 2016, hosted by the International Skin Imaging Collaboration (ISIC)

[15] Kawahara, Jeremy and Ghassan Hamarneh. “Multi-resolution-Tract CNN with Hybrid Pretrained and Skin-Lesion Trained Layers.” MLMI@MICCAI (2016).

[16] Anas, M.N., Gupta, R.K., & Ahmad, D.S. (2017). Skin Cancer Classification Using K-Means Clustering.

[17] Qaisar Abbas, M. E. Celebi, Carmen Serrano, Irene FondóN GarcíA, and Guangzhi Ma. 2013. Pattern classification of dermoscopy images: A perceptually uniform model. Pattern Recogn. 46, 1 (January 2013), 86-97.

[18] Almansour, Ebtihal and M. Arfan Jaffar. “Classification of Dermoscopic Skin Cancer Images Using Color and Hybrid Texture Features.” (2016).

[19] C. Ding and D. Tao, "Robust Face Recognition via Multimodal Deep Face Representation," in IEEE Transactions on Multimedia, vol. 17, no. 11, pp. 2049-2058, Nov. 2015.

[20] Tschandl P., Rosendahl C. & Kittler H. The HAM10000 dataset, a large collection of multi-source dermatoscopic images of common pigmented skin lesions. Sci. Data 5, 180161 doi.10.1038/sdata.2018.161 (2018)

[21] Noel C. F. Codella, David Gutman, M. Emre Celebi, Brian Helba, Michael A. Marchetti, Stephen W. Dusza, Aadi Kalloo, Konstantinos Liopyris, Nabin Mishra, Harald Kittler, Allan Halpern: “Skin Lesion Analysis Toward Melanoma Detection: A Challenge at the 2017 International Symposium on Biomedical Imaging (ISBI), Hosted by the International Skin Imaging Collaboration (ISIC)”, 2017; arXiv:1710.05006.

[22] Karel Zuiderveld. 1994. Contrast limited adaptive histogram equalization. In Graphics gems IV, Paul S. Heckbert (Ed.). Academic Press Professional, Inc., San Diego, CA, USA 474-485.

[23] A. Gijsenij, T. Gevers and J. van de Weijer, "Computational Color Constancy: Survey and Experiments," in IEEE Transactions on Image Processing, vol. 20, no. 9, pp. 2475-2489, Sept. 2011.

[24] Etta D, Pisano, S. Zong, R. E Jhonston “Contrast limited adaptive histogram equalization image processing to improve the detection of simulated speculation in Dense Monograms”, Journal of Digital Imaging, vol. 11, No. 4, pp 193-200, 1998

[25] Reza, A.M. The Journal of VLSI Signal Processing-Systems for Signal, Image, and Video Technology (2004) 38: 35.

[26] Beucher, Serge & De Morphologie Mathmatique, Centre. (2000). The Watershed Transformation Applied To Image Segmentation. Scanning. Microsc.. 6.

[27] Abbasi, N.R., Shaw, H.M., Rigel, D.S., Friedman, R.J., McCarthy, W.H., Osman, I., Kopf, A.W. and Polsky, D., 2004. Early diagnosis of cutaneous melanoma: revisiting the ABCD criteria. Jama, 292(22), pp.2771-2776.

[28] Simonyan, K. & Zisserman, A. (2014), 'Very Deep Convolutional Networks for Large-Scale Image Recognition', CoRR abs/1409.1556 .

[29] He, K., Zhang, X., Ren, S. & Sun, J. (2015). Deep Residual Learning for Image Recognition.. CoRR, abs/1512.03385.

[30] Alex Krizhevsky, Ilya Sutskever, and Geoffrey E. Hinton. 2012. ImageNet classification with deep convolutional neural networks. In Proceedings of the 25th International Conference on Neural Information Processing Systems - Volume 1 (NIPS'12), F. Pereira, C. J. C. Burges, L. Bottou, and K. Q. Weinberger (Eds.), Vol. 1. Curran Associates Inc., USA, 1097-1105.

[31] J. Almotiri, K. Elleithy and A. Elleithy, "Comparison of autoencoder and Principal Component Analysis followed by neural network for e-learning using handwritten recognition," 2017 IEEE Long Island Systems, Applications and Technology Conference (LISAT), Farmingdale, NY, 2017, pp. 1-5.